A&A 498, L25–L28 (2009)
DOI: 10.1051/0004-6361/200811476

Astronomy & Astrophysics

Letter to the Editor

Search for diffuse gamma rays from the Galactic anticentre region above 100 GeV with CELESTE

R. J. Britto[1,⋆], A. Jacholkowska[1,⋆⋆], F. Piron[1], E. Brion[2], J. Bussons Gordo[1,⋆⋆⋆], G. Debiais[3], B. Fabre[3,†], J. Lavalle[1,‡], F. Münz[4,§], E. Nuss[1], R. C. Rannot[2,¶], and T. Reposeur[2]

[1] Laboratoire de Physique Théorique et Astroparticules, Université Montpellier 2, CNRS/IN2P3, 34095 Montpellier, France
e-mail: Richard.Britto@lpta.in2p3.fr
[2] CENBG, Université Sciences et Techniques Bordeaux 1, CNRS/IN2P3, 33175 Gradignan, France
[3] Laboratoire de Physique Appliquée et Automatique, Université de Perpignan "via Domitia", 66860 Perpignan, France
[4] AstroParticule et Cosmologie, Université Denis Diderot-Paris 7, CNRS/IN2P3, CEA, Observatoire de Paris, 75205 Paris, France

Received 5 December 2008 / Accepted 23 February 2009

ABSTRACT

Context. Located in the French Pyrénées, CELESTE was the first ground-based γ-ray telescope with an energy threshold below 100 GeV. It acquired data from 1999 to 2004, and allowed flux measurements of the Crab nebula and the blazars Mrk 421 and Mrk 501.
Aims. We search for Galactic diffuse γ-ray emission, which is most significant around the Galactic plane, for $b = [-5°, +5°]$.
Methods. By using the significant data set available for the Crab nebula, we selected Crab OFF-source data at various Galactic latitudes, in order to analyse the diffuse emission. Selection criteria were applied to the sky position, atmospheric conditions, and detector stability.
Results. We obtained 108 mn of data in the Galactic anticentre region, providing the first upper limits of around 100 GeV to the diffuse γ-ray emission with atmospheric Cherenkov detectors. These limits are $\phi_{\rm int}^{\rm UL}(E > 140\ {\rm GeV}) = 9.4 \times 10^{-3}\ {\rm m^{-2}\ s^{-1}\ sr^{-1}}$ and $\phi_{\rm int}^{\rm UL}(E > 120\ {\rm GeV}) = 1.2 \times 10^{-2}\ {\rm m^{-2}\ s^{-1}\ sr^{-1}}$.

Key words. gamma rays: observations – methods: data analysis – methods: statistical – radiation mechanisms: non-thermal

1. Introduction

Galactic diffuse γ rays are produced by charged cosmic rays interacting with gas or photons in the interstellar medium. Most of these interactions occur in the Galactic plane: high energy γ rays experience weak attenuation and propagate without deviation from their production regions, due to their neutrality. These γ rays can therefore be used to infer the spatial distribution, propagation, and energy distributions of charged cosmic rays.

Previous measurements of the Galactic diffuse emission were obtained by the EGRET experiment aboard CGRO between 30 MeV and ~50 GeV, leading to the localisation of this emission between $[-5°, +5°]$ of Galactic latitude (Hunter et al. 1997). The ground-based telescopes Whipple (LeBohec et al. 2000), HEGRA (Aharonian et al. 2001), TIBET (Amenomori et al. 2006), and CANGAROO (Ohishi 2005) provided upper limits (ULs) at energies above 500 GeV for different regions of the Galactic plane. Milagro detected a signal above 3.5 TeV with a significance level of 4.5σ for a Galactic longitude $40° < l < 100°$, and inferred an UL in the same energy range for $140° < l < 200°$ (Atkins et al. 2005). These two regions are located at $-5° < b < +5°$. HESS reported a diffuse flux above 170 GeV around the Galactic centre (Aharonian et al. 2006).

CELESTE observed the Galactic anticentre region around the Crab nebula in an energy domain previously uncovered. This region is part of the $140° < l < 200°$ Milagro region. We consider in our study two models of cosmic-ray interactions with the interstellar medium (Strong et al. 2000, 2004). These models reproduce the EGRET data and infer, after normalization with the Galactic anticentre flux at 10 GeV, the following photon flux:

$$\frac{{\rm d}\phi}{{\rm d}S\ {\rm d}t\ {\rm d}\Omega\ {\rm d}E} = 8.3 \times 10^{-4} \left(\frac{E}{10\ {\rm GeV}}\right)^{-\Gamma}\ {\rm m^{-2}\ s^{-1}\ sr^{-1}\ GeV^{-1}} \quad (1)$$

where Γ is the differential index, which respectively equals 2.0 and 2.5, for the two considered models valid between ~10 and 400 GeV.

In Sect. 2, we present the CELESTE setup and the preliminary phase of the signal extraction. In Sect. 3, we describe the analysis procedure, using Monte Carlo simulations and a composed discriminating variable. In Sect. 4, we provide our results and the ULs obtained in the search for diffuse γ rays, and in Sect. 5 we present our conclusions.

2. The CELESTE experiment

Located in the Eastern French Pyrénées (42.50° N, 1.97° E, altitude: 1650 m), CELESTE (for "C(h)Erenkov Low Energy

⋆ *Current address*: Department of High Energy Physics, Tata Institute of Fundamental Research, Mumbai-400 005, India
⋆⋆ *Current address*: LPNHE, Université Pierre et Marie Curie-Paris 6, Université Denis Diderot-Paris 7, CNRS/IN2P3, Paris, France
⋆⋆⋆ *Current address*: Departamento de Fisica, Universidad de Murcia, 30080 Murcia, Spain
† Deceased
‡ *Current address*: Dipartimento di Fisica Teorica, Universitá degli Studi di Torino, via Giuria 1 - mailbox 150, 10125 Torino, Italy
§ *Current address*: Instituto di astrofisica spaziale e fisica cosmica, via P. Gobetti 101, 40129 Bologna, Italy
¶ *Current address*: Astrophysical Sciences Division, Bhabha Atomic Research Centre, Mumbai-400 085, India

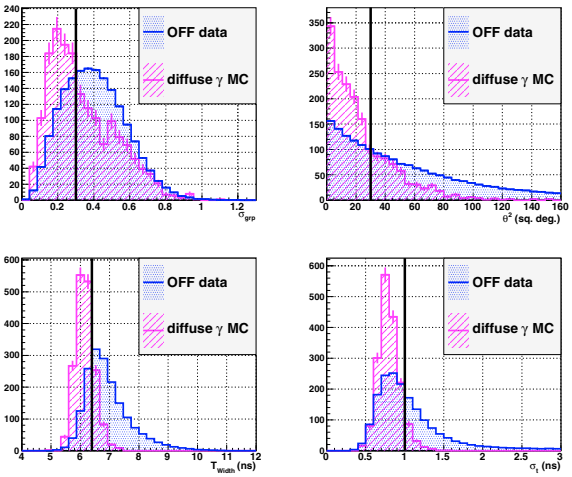

Fig. 1. Distributions of the four discriminating variables. OFF data (dotted blue)/MC diffuse γ-ray with $\Gamma = 2.5$ (hatched magenta) comparison. Discrimination between hadrons and diffuse γ rays is possible.

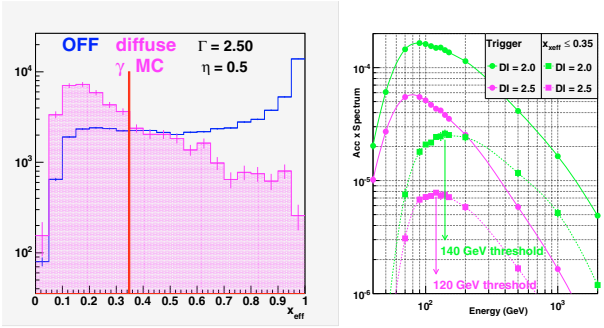

Fig. 2. *Left*: distributions of $x_{\rm eff}$ for OFF data and simulated diffuse γ rays for the $\Gamma = 2.5$ spectral index. The vertical bar indicates the $x_{\rm eff} = 0.35$ cut of our analysis. *Right*: CELESTE differential rate for diffuse γ rays in the anticentre region after trigger and after $x_{\rm eff}$ analysis for $\Gamma = 2.0$ (red lines) and $\Gamma = 2.5$ (green lines) respectively.

Sampling and Timing Experiment") used 40 initially, later 53, of the 54 m^2 mirrors (called heliostats) of the Thémis former solar plant between 1999 and 2004, and was operated during clear, moonless nights (Paré et al. 2002). A γ ray entering the atmosphere creates an electromagnetic cascade of photons and relativistic electrons and positrons, which cause Cherenkov radiation as they travel faster than the speed of light in the lower atmospheric layers. The blue Cherenkov pool on the ground is reflected by the heliostats to secondary optics and then to photomultipliers (one per heliostat), positioned at the top of the 100 m tower. Winston cones in front of the photomultipliers provided a 0.°57 field of view diameter to the telescope, which corresponds to the apparent diameter of the atmospheric showers. Large collection area and fast acquisition electronics system (~940 MHz) for sampling the Cherenkov pulses allowed CELESTE to be the first ground-based Cherenkov telescope with a trigger threshold of below 100 GeV (de Naurois et al. 2002).

To decrease the incidence of random triggers by night sky background light, trigger conditions were applied, using a setup of 5 trigger groups of 8 heliostats each[1]. We usually insisted on a majority of 3 groups being above a threshold of 4.5 photoelectrons per heliostat.

Because of the large isotropic background originating from the showers induced by charged cosmic rays (protons, electrons, ions), point source data were taken in ON/OFF pairs, i.e., by pointing the telescope in the source direction (ON) and away from the source sky region (OFF). The OFF data acquired was usually associated with γ-ray source data acquisitions by shifting them by +20 or –20 mn in right ascension in order to follow the same path in the sky. Due to differences in atmospheric conditions between ON and OFF acquisitions, a padding procedure was applied to balance the noise in each channel between the two data sets. A software trigger was then applied, with a more severe trigger condition, to reject low-charge event excess.

The data analysis was based on the geometric and timing properties of the Cherenkov wavefront, which allow discrimination between electromagnetic and hadronic showers. A significant excess in the ON-OFF subtraction was then able to be interpreted as a γ-ray signal.

[1] Data used for the analysis presented in this paper are from the 40 heliostat period (1999–2001). See Smith et al. (2006) for more details on the 53-heliostat setup.

3. Analysis procedure

The search for diffuse γ rays at low Galactic latitudes with CELESTE was completed by using OFF source data only, comparing data taken near and away from the Galactic plane. The Crab OFF-source observations provided a large sample of data, some close to the Galactic plane (OFF$_1$) and others in its periphery (OFF$_2$). In the ON-OFF method presented in Sect. 2, "ON" data are replaced here by the closest OFF region to the Galactic equator, and "OFF" by a farther region, in order to perform a OFF$_1$-OFF$_2$ analysis (Britto et al. 2007).

3.1. Monte Carlo simulations

Accurate Monte Carlo (MC) simulations are necessary in detector calibration, to reproduce both the signal signature and trigger rate. The atmospheric showers were simulated by CORSIKA 4.50 (Heck & Knapp 2001) adapted for CELESTE. Optics and electronics were simulated by specific C++ software developed by the collaboration (Münz 2003; Smith et al. 2006).

The signal that we extract is characterized by comparing the distributions of the discriminating variables $\sigma_{\rm grp}$, θ^2, $T_{\rm Width}$, and $\sigma_{\rm t}$, which represent, respectively, the uniformity of the Cherenkov pool on the ground, the reconstructed direction of the shower, the time width of the wavefront, and the signal arrival time dispersion (Britto 2006). Distributions are presented after preliminary cuts, i.e., mainly after applying a software trigger.

The MC simulations of a γ-ray point source reproduce the Crab signal obtained by ON-OFF subtraction (de Naurois et al. 2002; Britto 2006). This good agreement between our simulations and true data allowed us to optimize the hadron rejection cuts for different diffuse emission models by simulating the corresponding spectra. Figure 1 was obtained after preliminary analysis cuts, when OFF data were mostly dominated by protons and helium nuclei, and illustrates the discrimination between diffuse γ-ray signal and hadrons.

Finally, protons and helium nuclei were simulated in attempting to provide the proper physical background and reproduce the total trigger rate of the experiment (most often between 20 and 25 Hz). Raw data mainly consist of protons and helium nuclei, and the total trigger rate is almost reproduced, with a contribution at 13.4 Hz from protons, and at 3.5 Hz from helium nuclei (Britto 2006).

Table 1. CELESTE sensitivity to the diffuse signal for the spectral models of Eq. (1) and an observation time of 10h, in case of no diffuse signal expected in the OFF_2 region.

Γ	n_γ (min^{-1})	Q	N_σ for T_{obs} = 10 h
2.0	1.45 ± 0.03	1.39	0.9
2.5	0.36 ± 0.01	0.96	0.2

3.2. Sensitivity to diffuse γ rays

To improve the sensitivity of our analysis, a composite discriminating variable ($x_{\rm eff}$) was used for γ-ray identification. It was developed from probability density functions (PDFs) of the three uncorrelated discriminating variables $\sigma_{\rm grp}$, θ^2, and $T_{\rm Width}$, which were computed from γ-ray MC simulations and OFF data in representing the diffuse γ-ray signal and the hadronic background respectively. These PDFs were obtained from the distributions shown in Fig. 1. The $x_{\rm eff}$ variable is defined to be:

$$x_{\rm eff} = \frac{\eta \times \prod_{i=1}^{n} g_{\rm bckg}(x_i)}{(1-\eta) \times \prod_{i=1}^{n} g_{\rm signal}(x_i) + \eta \times \prod_{i=1}^{n} g_{\rm bckg}(x_i)}, \quad (2)$$

where η is a weight factor, whose value is fixed to be 0.5, x_i is the discriminating variable i, and $g_{\rm bckg/signal}$ are the PDFs. As shown in Fig. 2 (left), $x_{\rm eff}$ distributions reach a peak close to 0 for γ-ray (1 for hadronic) events.

The sensitivity of our analysis was determined by the quality factor Q, which is a function of the efficiencies of the diffuse signal (ϵ_γ, computed using simulations) and background ($\epsilon_{\rm b}$), after analysis cuts to $x_{\rm eff}$: $Q = \frac{\epsilon_\gamma}{\sqrt{\epsilon_{\rm b}}}$. The significance of the expected diffuse signal was then:

$$N_\sigma \simeq Q \times \frac{n_\gamma}{\sqrt{2\, n_{\rm OFF}}} \times \sqrt{T_{\rm obs}}, \quad (3)$$

where n_γ is the diffuse γ-ray rate, $n_{\rm OFF} \sim 25$ Hz is the hadron rate, and $T_{\rm obs}$ is the observation time.

We compared the $x_{\rm eff}$ distributions of two sets of diffuse γ-ray simulations for $\Gamma = 2.0$ and 2.5 with the Crab OFF data at Galactic latitudes close to $l = -10°$ (in order to represent the OFF_2 region). Distributions for $\Gamma = 2.5$ are given in Fig. 2 (left). For each spectral index, the cut $x_{\rm eff} \leq 0.35$ provides the best quality factor Q, and hence the most effective hadronic rejection. The corresponding significances for a collection time of 10 h are presented in Table 1.

From this table, one can see that conventional models of diffuse γ-ray emission do not predict an easy detection with CELESTE from the available data sets. However, the lack of observations around 100 GeV still infers that this analysis is interesting.

3.3. Analysis threshold

The CELESTE effective area for a diffuse signal $A_{\rm eff}(E)$ (in m^2 sr) was computed at several energies E, as follows:

$$A_{\rm eff}(E) = 2\pi \int_0^{R_{\rm max}} \int_0^{\Omega_{\rm max}} P(E,R,\theta) R {\rm d}R {\rm d}\Omega, \quad (4)$$

where $P(E,R,\theta)$ is the trigger probability, R is the distance between the injection shower point and the pointing axis, and Ω is the solid angle defined by the incident angle θ of the primary γ ray.

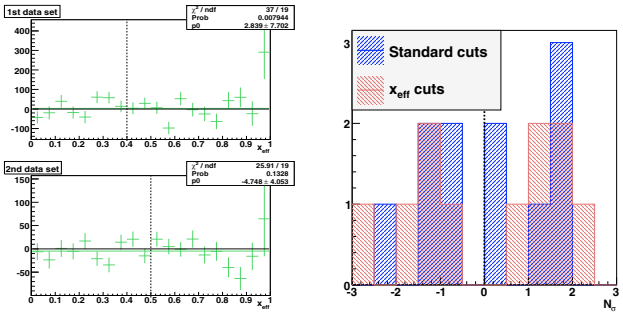

Fig. 3. *Left*: Markarian 421 and 501 OFF-OFF distributions of $x_{\rm eff}$ for two different data sets. Q is maximum for $x_{\rm eff} \leq 0.4$ (resp. 0.5) for the data from two different pointing configurations. Fits with a constant show the compatibility with zero of the distributions. *Right*: distributions of the significances for the 11 pairs of this selection. Comparison is done between our $x_{\rm eff}$ analysis and standard separate cuts on the discriminating variables.

The CELESTE differential rate is the product of the effective area with the spectrum model $\phi(E)$ and the expectations for the two spectral models are shown in Fig. 2 (right) as a function of the energy for the two spectral models (Eq. (1)). The points obtained from MC are connected with each other by smoothed lines. The two upper ones correspond to trigger events, and the two lower ones are obtained after applying the analysis cuts. The energy threshold is defined by convention to be the maximum of the differential rate. It reaches 80 GeV at the trigger level for the two spectral indices, and 140 GeV for $\Gamma = 2.0$ (120 GeV for $\Gamma = 2.5$) after analysis cuts.

4. Results

4.1. Data selection and validation of the method

The data used in the following analysis were selected with criteria based on atmospheric and acquisition stabilities. We required a similar path on the sky for the two OFF members of a same pair, which is only possible if they have the same declination. These standard run selections are similar to those presented by Smith et al. (2006) and Lavalle et al. (2006).

A preliminary check of the OFF-OFF analysis consisted of verifying that there was no significant systematic effect in the OFF pair association of data taken at different dates (yet at the same local coordinates on the sky). We used the OFF data associated with the Mrk 421 and Mrk 501 blazars, since no signal was expected at these high Galactic latitude regions. PDFs were compiled according to the location of these sources on the sky. Figure 3 shows that the OFF-OFF analysis presented here yields significances that are consistent with 0 for the 11 selected pairs (corresponding to 150 mn of data) where no signal is expected. In the right panel, we also compare our $x_{\rm eff}$ analysis results with those of the standard analysis completed by applying a separate cut to each variable (de Naurois et al. 2002).

4.2. OFF-OFF analysis in the anticentre region

We analysed OFF data acquired at different dates in searching for an event excess close to the Galactic equator. We used a set of OFF data associated with Crab nebula observations, where the "OFF_1" data were located at Galactic latitude $l \simeq -2°$ and "OFF_2" data at $l \simeq -10°$, for a given declination. An

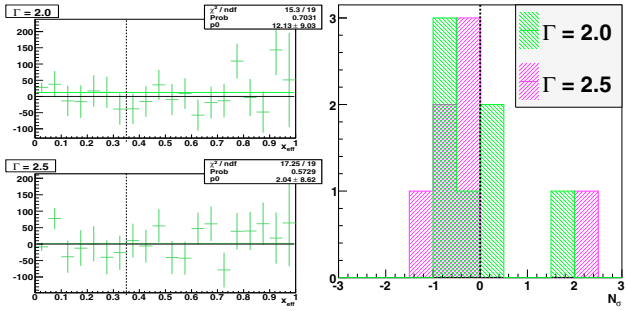

Fig. 4. *Left*: Crab OFF-OFF distributions of $x_{\rm eff}$ in the search of diffuse γ rays in the anticentre region, obtained with PDFs adapted to the assumed spectral index: $\Gamma = 2.0$ (*upper panel*) and $\Gamma = 2.5$ (*lower panel*). Q is maximum for $x_{\rm eff} \leq 0.35$ for both the Γ values. Fits with a constant show the compatibility with zero of the distributions. *Right*: distributions of the significances of the 7 pairs of the Galactic diffuse γ-ray selection, for $\Gamma = 2.0$ and 2.5.

Table 2. Analysis results for the 7 pairs of the Crab OFF selection.

	Raw data	Prelim. cuts	Standard cuts	$x_{\rm eff} \leq 0.35$ cut $\Gamma = 2.0$	$\Gamma = 2.5$
$N_{\rm OFF_1}$	169 869	34 863	3131	6763	7337
$N_{\rm OFF_2}$	168 499	34 692	3147	6737	7383
$N_{\rm OFF_1} - N_{\rm OFF_2}$	–	–	-16 ± 71	26 ± 92	-46 ± 94
N_σ	–	–	–0.17	0.17	–0.32

$\rm OFF_1$–$\rm OFF_2$ analysis was performed in attempting to detect a γ-ray excess, which was expected to be the most intense close to the Galactic equator. We selected 7 pairs, corresponding to 108 mn of data. Figure 4 (left) shows the $x_{\rm eff}$ distributions after preliminary cuts. Diffuse γ-ray PDFs were used for $\Gamma = 2.0$ and 2.5. The $x_{\rm eff} \leq 0.35$ cut applied to this data sample yields no significant signal (Table 2 and Fig. 4, right).

4.3. Upper limit on the diffuse γ-ray emission

The diffuse emission in the $\rm OFF_2$ region is expected to be non-negligible and equal to 66% of that in the $\rm OFF_1$ region, assuming the same spatial distribution as measured by EGRET (Hunter et al. 1997, Fig. 3d). Taking this contribution into account and using Eq. (3), two 95% C.L. upper limits to the γ-ray flux from the Galactic anticentre region were obtained: 23.1 γ/ min for $\Gamma = 2.0$ and 33.5 γ/ min for $\Gamma = 2.5$. By comparing these limits with the outputs of Eq. (3), the integration of Eq. (1) yields the following limits to the integral photon fluxes:

$$\phi_{\rm int}^{\rm UL}(E > 140\ {\rm GeV}) = 9.4 \times 10^{-3}\ {\rm m^{-2}\ s^{-1}\ sr^{-1}},\ \text{for}\ \Gamma = 2.0 \quad (5)$$

$$\phi_{\rm int}^{\rm UL}(E > 120\ {\rm GeV}) = 1.2 \times 10^{-2}\ {\rm m^{-2}\ s^{-1}\ sr^{-1}},\ \text{for}\ \Gamma = 2.5. \quad (6)$$

These ULs are plotted in Fig. 5. The main systematic effects on flux measurements originate in the uncertainties in the atmospheric transmission and the optical throughput of the experiment. They were estimated to be less than 25% (Smith et al. 2006). Furthermore, we tested the stability of our results by varying the η parameter (see Eq. (2)) within a reasonable range and by applying various selection cuts to $x_{\rm eff}$ around the nominal value of 0.35. Figure 5 also shows the measurements and ULs obtained by other experiments observing the Galactic anticentre region in the energy range between 1 GeV and 10 TeV.

5. Conclusions

CELESTE was the first ground-based Cherenkov detector with an energy threshold below 100 GeV. Although we had much

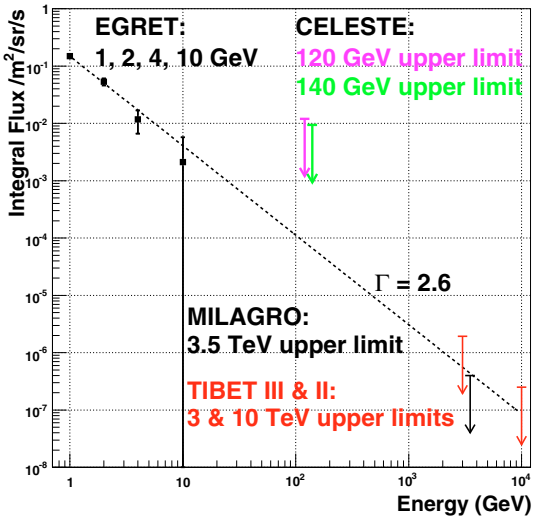

Fig. 5. CELESTE 120 and 140 GeV ULs on the diffuse γ-ray emission toward the Galactic anticentre direction. EGRET data in the ($l \simeq 190°$, $|b| < 2°$) region are displayed, as well as the upper limits obtained with the Milagro experiment in the ($140° < l < 200°$, $|b| < 5°$) region (Atkins et al. 2005), and with the Tibet II and III experiment in the ($140° < l < 255°$, $|b| < 2°$) region (Amenomori et al. 2006).

OFF data available to us that is associated with the Crab nebula, the absence of dedicated observations to search for diffuse emission left us with 108 mn of usable data. No significant signal was detected in the Galactic plane. However, our study illustrates that CELESTE is the only experiment so far to have provided upper limits to the diffuse γ-ray emission from the Galactic anticentre region around 100 GeV.

Our study provides a favorable perspective in our continuing search for the diffuse emission with other Cherenkov atmospheric detectors. Next-generation Cherenkov telescopes such as HESS II (Vincent et al. 2004), MAGIC II (Baixeras et al. 2005), and MACE (Koul et al. 2005) are expected to be sensitive enough to detect diffuse γ-ray emission with an energy threshold of as low as 20 GeV, to complement the surveys completed with the AGILE, GLAST and AMS-02 space detectors.

References

Aharonian, F. A., Akhperjanian, A. G., Barrio, J. A., et al. 2001, A&A, 375, 1008
Aharonian, F., Akhperjanian, A. G., Bazer-Bachi, A. R., et al. 2006, Nature, 439, 695
Amenomori, M., Ayabe, S., Bi, X. J., et al. 2006, Proc. 20th ECRS in Lisbon, [arXiv:astro-ph/0611335]
Atkins, R., Benbow, W., Berley, D., et al. 2005, Phys. Rev. Lett., 95, 251103
Baixeras, C., et al. 2005, Proc. 29th ICRC, Pune, 5, 227
Britto R. 2006, Thèse de Doctorat de l'Université Montpellier II http://tel.archives-ouvertes.fr/tel-00358634/fr/
Britto, R. for the CELESTE Coll. 2007, Proc. SF2A-2007, Grenoble, France
Heck, D., & Knapp, J. 2001, CORSIKA: A User's Guide (Version 6.005), Forschungszentrum Karlsruhe GmbH
Hunter, S. D., Bertsch, D. L., Catelli, J. R., et al. 1997, ApJ, 481, 205
Koul, R., et al. 2005, Proc. 29th ICRC, Pune, 5, 243
Lavalle, J., Manseri, H., Jacholkowska, A., et al. 2006, A&A, 450, 1
LeBohec, S., Bond, I. H., Bradbury, S. M., et al. 2000, ApJ, 539, 209
Münz F. 2003, Thèse de Doctorat des Universités Paris VII/Charles de Prague, http://tel.archives-ouvertes.fr/tel-00003334/fr/
de Naurois, M., Holder, J., Bazer-Bachi, R., et al. 2002, ApJ, 566, 343
Paré, É., Balauge, B., Bazer-Bachi, R., et al. 2002, NIM, A490, 71
Ohishi, M., et al. 2005, Proc. 29th ICRC, Pune, 4, 39
Smith, D. A., Brion, E., Britto, R., et al. 2006, A&A, 459, 453
Strong, A. W., Moskalenko, I. V., & Reimer, O. 2000, ApJ, 537, 763
Strong, A. W., Moskalenko, I. V., & Reimer, O. 2004, ApJ, 613, 962
Vincent, P., and the HESS Coll 2004, Proc. SF2A-2004, Paris, France